

# Goethite Nanofibers /CNTs based Nanocomposites Synthesized by Free-Template Hydrothermal Method and their Physico-Chemical Properties for Energy Storage Application

Sara Djelamda, Fahima Djefafliya, Aicha Harat, Aissa Nait-Merzoug, Damilola Momodu, Ncholu Manyala,

Mohamed Guerioune and Ouanassa Guellati

**Abstract**—In this investigation, we report the synthesis of Goethite-NFs/CNTs nanocomposites using hydrothermal method at optimized growth condition. These nanostructured products have been characterized in order to identify their physico-chemical properties by different techniques, such as X-Ray Diffraction (XRD), Raman Spectroscopy, High Resolution Scanning Electron Microscopy (FESEM), Thermal analysis (TGA/DTA) and UV- Vis Spectroscopy. The obtained Goethite nanofibers (NFs) have shown structured triangular base nanofibers with diameter in the range [181 - 363 nm]. Using nested and twisted CNTs (MWNTs type) but fairly homogeneous in diameter around 48 nm, the formation of an assembly of two forms (MWNTs and iron oxide Nanofibers) in nanocomposite configuration confirms the significant improvement of their physico-chemical properties, like the increase in their electrical conductivity proven by their obtained gap energy  $E_g$  from 3.12 to 2.50 eV. Consequently, the reached results prove clearly that this kind of iron oxide-NFs/MWNTs based nanocomposites can be excellent candidate as electroactive nanomaterials for energy storage application.

**Keywords**— Nanotechnology, Iron Hydroxide/Oxide, Hydrothermal Process, Optical Properties, Gap Energy.

## I. INTRODUCTION

Energy field is one of the most important prospects that have been highlighted in last years. Therefore, the energy storage is considered as nature friend and in order to face the ever-assisted energy crisis, scientists are seeking to find storage devices with high efficiency and low cost production [1, 2].

Additionally, transition metal oxides based on Ni, Mn, Fe or Co, with variable oxidation states are among the incoming materials that have many applications due to their multiple advantages, such as : optical and energy-storage devices, biomedical and biotechnological fields [3-5]. Nowadays, iron oxides/hydroxides are widely and increasingly used in many applications, much more in biomedical, waste water treatment, energy storage and optical devices due to their super-

paramagnetic, safety, low cost synthesis and high electrical conductivity properties [3, 5-8]. More specifically, among them there is hematite ( $\alpha$ - $\text{Fe}_2\text{O}_3$ ), maghemite ( $\gamma$ - $\text{Fe}_2\text{O}_3$ ), magnetite ( $\text{Fe}_3\text{O}_4$ ), bixbyite ( $\text{b-Fe}_2\text{O}_3$ ) and wustite ( $\text{FeO}$ ) as oxides; whereas hydroxides like oxy-hydroxide ( $\text{Fe}(\text{OH})_2$ ,  $\text{Fe}(\text{OH})_3$  and mineral goethite ( $\text{FeOOH}$ )) [9-11]. Hematite is thermodynamically the more stable mineral than others in the presence of oxygen [11, 12] and evinces, strong electron–electron correlations and electron–photon coupling showing interesting optical properties due to their unique complex electronic structures [13]. However, Magnetite ( $\text{Fe}_3\text{O}_4$ ) is used in many fields due to their unique nature and it contains both secondary (II) and tertiary iron (III) [14, 15]. For iron based hydroxides case, Goethite ( $\alpha$ - $\text{FeOOH}$ ) is one of the most wide spread minerals in the soil, with an orthorhombic structure illustrating the most stable iron hydroxide. It turns into hematite at 300°C [16-18].

Moreover, Goethite is used with reduced Graphene Oxide to remove lead from wastewater via adsorption technique. The lead ion is considered one of the most dangerous metals, as it affects several systems, such as nervous system, digestive system, kidneys, heart and blood vessels [19]. On the other hand, Biochar-supported Al-Substituted Goethite (BAG) is used also as a new absorbent in order to get rid of polluted nitrates in groundwater [20]. More importantly, Huan Xu and al. found that the specific capacitance of alpha-iron oxy-hydroxide/reduced Graphene oxide ( $\alpha$ - $\text{FeOOH}/\text{rGO}$ ) composites is around 452  $\text{F.g}^{-1}$  obtained at a current density 1  $\text{A.g}^{-1}$  [21]. On the other hand, Rasmita Barika found that the specific capacitance is equal to 160  $\text{F.g}^{-1}$  for  $\alpha$ - $\text{FeOOH}$  [22]. Furthermore, nanocomposites are a combination of massive matrix with nanometric reinforcement with new properties resulting from structural and chemical combination. Thus, in this investigation we report the successful fabrication of Goethite-NFs/CNTs nanocomposites using hydrothermal technique at optimized growth condition. These nanostructured products have been characterized in order to

*Manuscript received October 9, 2022; revised July 5, 2023.*

S. Djelamda is with Mohamed Chérif Messaadia University, BP. 1553, Souk-Ahras 41000, ALGERIA. (e-mail: [saradjelamda1996@gmail.com](mailto:saradjelamda1996@gmail.com))

F. Djefafliya, A. Nait-Merzoug and O. Guellati are with Mohamed Chérif Messaadia University, BP. 1553, Souk-Ahras 41000, ALGERIA and LERC Laboratory, Physic Department, Badji Mokhtar University of Annaba, BP. 12, Annaba 23000, ALGERIA. (e-mails: [djefafliyahima@gmail.com](mailto:djefafliyahima@gmail.com), [abenlala@yahoo.fr](mailto:abenlala@yahoo.fr) and [guellati23@yahoo.fr](mailto:guellati23@yahoo.fr))

A. Harat and M. Guerioune are with LERC Laboratory, Physic Department, Badji Mokhtar University of Annaba, BP. 12, Annaba 23000, ALGERIA. (e-mails: [harat\\_aicha@yahoo.fr](mailto:harat_aicha@yahoo.fr) and [mguerioune@yahoo.fr](mailto:mguerioune@yahoo.fr))

D. Momodu and N. Manyala are with Department of Physics, Institute of Applied Materials, SARChI Chair in Carbon Technology and Materials, University of Pretoria, Pretoria 0028, SOUTH AFRICA. (emails: [dymomodu@yahoo.com](mailto:dymomodu@yahoo.com), [ncholu.manyala@up.ac.za](mailto:ncholu.manyala@up.ac.za))

Digital Object Identifier (DOI): 10.53907/enpesj.v3i1.159

identify their physico-chemical properties for specific energy application fields. Consequently, oxygen functionalized MWNTs (O-MWNTs) can be a real choice because of their low-cost local production and their lower impact on the environment compared with other materials in different application field. In addition, the local synthesized MWNTs used in this work possess interesting characteristics (structural, textural and chemical) for later application, such as : high purity around 98%, high selectivity, oxygen based functional groups and specific surface area around 150 m<sup>2</sup>/g.

## II. EXPERIMENTAL PROCEDURE

### A. Goethite/CNTs synthesis

The experimental protocol implemented during the synthesis of iron oxide based products with and without the presence of CNTs (MWNTs type synthesized in LEREC laboratory [23]) using hydrothermal process goes through the following stages : firstly, we dispersed an iron precursor (FeCl<sub>2</sub>.4H<sub>2</sub>O) (with or without CNTs) in distilled water under magnetic stirring “250 rpm” for 30 min. Then, a quantity of NaOH was added slowly under stirring for 10 min. Secondly, the resulting orange (or blacked orange in the presence of CNTs) solution was introduced into an 40 mL Teflon-lined hydrothermal autoclave system which has been kept at 120°C in a furnace for 18 h. Lastly, after cooling down naturally to room temperature, the obtained products were always washed, rinsed with distilled water and filtered several times until a neutral pH.

### B. Characterization techniques

X-Ray Diffraction (XRD) spectra have been obtained through the X' Pert PRO diffractometer (PANalytical BV, Netherlands) with theta/theta geometry operating from an anticathode source Co-K $\alpha$  ( $\lambda= 1.79 \text{ \AA}$ ) at 35 kV voltage and 50 mA current in the  $2\theta$  range [5-90°]. Raman spectra of the samples were recorded on a Jobin Yvon Horiba TX 6400 micro-Raman spectrometer excited with 514 nm line of an argon laser with power energy 0.33 mW. The surface morphology of the pure Goethite (Fe<sub>2</sub>O<sub>3</sub>.H<sub>2</sub>O), carbon nanotubes (CNTs) and their nanocomposite (Goethite nanofibers/CNTs) were analyzed by field emission scanning electron microscopy (FESEM) Zeiss Ultra plus 55 at 2 kV accelerating voltage and high resolution transmission electron microscopy (TEM) carried out with a JEOL JEM-2100F microscope operated at 200 kV (Akishima-shi, Japan). Thermal analysis (TGA/DTA) was carried out using a Thermo Gravimetric Analysis instrument (TA Instruments Q600 Simultaneous (DSC/TG) analyzer). The temperature was increased from room temperature to 1000 °C with a heating rate of 10 °C.min<sup>-1</sup> under air atmosphere. However, the optical properties were performed by measuring the absorbance using UV-Vis spectrophotometer (Thermo Technical GENESYS 10S) with double beam in order to study the energy band gap of these products.

## III. RESULTS AND DISCUSSION

X-ray diffraction is most commonly used as a structural identification tool to characterize and to study the crystalline appearance of the synthesized products using the hydrothermal technique. Figure 1 illustrates the typical XRD patterns of synthesized Goethite nanostructures and their nanocomposite “Goethite/CNTs” using a free template hydrothermal method at optimized conditions. These diffractograms have been identified through their most intense

peaks which are always indexed using a standard (JCPDS) database. They clearly confirm the formation of an hydrated iron oxide phase (Fe<sub>2</sub>O<sub>3</sub>.H<sub>2</sub>O) equivalent of two Goethite (FeOOH) and its nanocomposite with MWNTs known via their characteristic peak at 26.77° corresponding (002) crystalline plan [00-058-1638] [24-26].

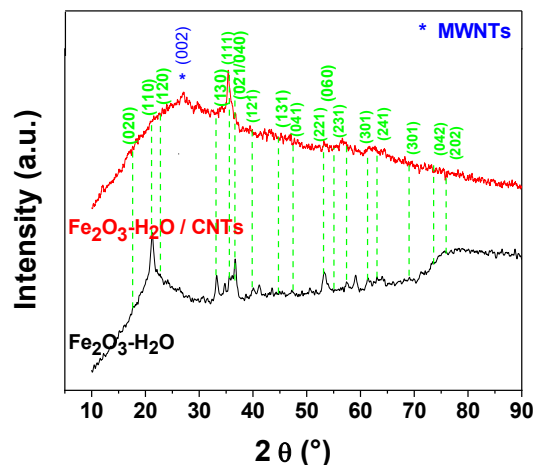


Fig. 1: XRD diffractograms of Goethite and their nanocomposite “Goethite/MWNTs”.

**Table. I**  
CALCULATED CRYSTALLINE PARAMETERS FOR HYDRATED IRON OXIDE (GOETHITE) SYNTHESIZED BY HYDROTHERMAL METHOD.

PHASE / REF.	a (Å)	b (Å)	c (Å)
Fe <sub>2</sub> O <sub>3</sub> .H <sub>2</sub> O (Goethite)	4.563	10.020	3.016
[00-002-0272]	4.587	9.937	3.015

However, the characteristic peaks of the Goethite type iron oxide phase (Fe<sub>2</sub>O<sub>3</sub>.H<sub>2</sub>O) for these two products are indexed to around 21.46°, 33.17° and 36.65° corresponding to the crystal planes (110), (130) and (111), respectively, which agrees with the previous results [27, 28]. This oxide phase has an orthorhombic structure according to the JCPDS card [00-002-0272]. Moreover, this Goethite phase nanostructure in the nanocomposite case showed a slight shift in the peaks position, which confirms its contact with MWNTs as a second phase.

In addition, the crystalline parameters of this synthesized hydrated iron oxide (Goethite) phase were calculated and shown in table I with values close to those of the JCPDS card [00-002-0272] as an identification reference. On the other hand, the estimated crystallinity degree of pure Goethite is around 23%; whereas it is around 16%, in the case of their nanocomposite with MWNTs.

In the same way, Raman spectroscopy is another technique used to obtain more information about the graphitization and the composition characteristics of the synthesized material. The Raman spectra of these products are illustrated in figure 2. As a result, in the case of the nanocomposite (Goethite/MWNTs), the Raman spectra present the main Raman vibration peaks around 219, 289, 372 and 689 cm<sup>-1</sup> corresponding the stretch bond vibrations found in Fe-O, Fe-OH, Fe-O-Fe and Fe-O oxides, respectively [3, 29, 30].

While, D and G band characteristic peaks corresponding the MWNTs formation are found around 1350/1575 cm<sup>-1</sup> (Fig. 2a) and 1348/1583cm<sup>-1</sup> (Fig. 2b), in pure (MWNTs) and nanocomposite (Goethite/MWNTs), respectively. The G band is a characteristic of the hybridization of carbon atoms

corresponding to tangential vibrations mode of elongation C-C bonds; which is generally a strong indication of the crystallinity/graphitization degree of carbon nanotubes.

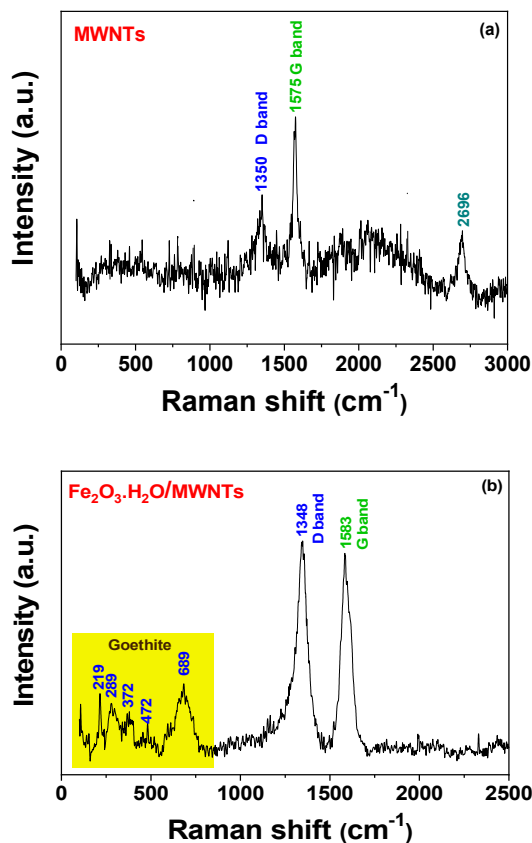


Fig. 2: Raman spectra of pure MWNTs (a) and their nanocomposite (b) (Goethite/MWNTs).

Otherwise, the D band is associated to the disorder in the tubular structure nanotubes where their intensity characterizing the defects concentration. However, the peak found around 2696  $\text{cm}^{-1}$  corresponds to the 2D band, as the second order harmonic of the D band, which can be used to differentiate the CNTs properties [31, 32, 33]. These peaks characterizing the used MWNTs are found shifted in the produced nanocomposite due to the incorporation of iron oxide nanostructure and their contact. Table II regroup the MWNTs peaks characteristics with and without Goethite nanostructure.

Table II

COMPARISON BETWEEN PEAKS POSITIONS AND THEIR RELATIVE INTENSITIES RATIO.

PRODUCT	D ( $\text{cm}^{-1}$ )	G ( $\text{cm}^{-1}$ )	$I_D/I_G$
MWNTs	1350	1575	0.52
Goethite/MWNTs	1348	1583	1.06

Moreover, we can notice an increase in the  $I_D/I_G$  ratio estimating the defect to twice in the nanocomposite (Goethite/MWNTs) case indicating their contact, which proves thereby the decrease found in the crystallinity degree estimated by XRD analysis.

**Thermal Characteristics:** In order to have idea on the Goethite concentration in the synthesized nanocomposite, we have also performed thermogravimetric analysis (TGA/DTA) under air where we have followed the weight loss evolution in function of oxidation temperature, as represented in figure 3. We can see two main oxidation peaks at 271 and 551  $^{\circ}\text{C}$  indicating the produced nanocomposite selectivity and purity.

The first peak corresponding temperature inferior to 300  $^{\circ}\text{C}$  clearly confirms the Goethite (hydrated iron oxide) transformation into iron oxide; however, 551  $^{\circ}\text{C}$  confirm the functionalized MWNTs combustion [34]. Moreover, this thermal spectra show that this nanocomposite is thermally stable beyond 600  $^{\circ}\text{C}$ . From TGA, the first loss around 6 wt.% is attributed to dehydroxylation of Goethite due to their transformation into hematite, as reported previously in the literature [35]. Nevertheless, the second loss around 20 wt.% is attributed to the oxidation of MWNTs by atmospheric oxygen or iron oxide second phase at around 551  $^{\circ}\text{C}$  which is also consistent with work found in Debski's team publication [26].

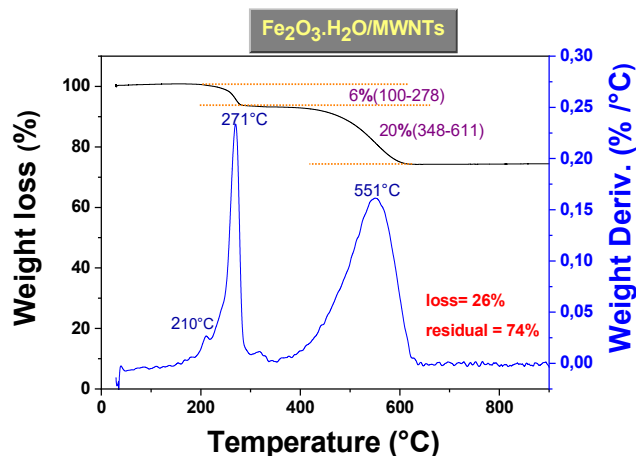


Fig. 3: Thermal analysis (TGA/DTA) of Goethite/MWNTs nanocomposite produced by hydrothermal process.

From these TA analysis curves, we can conclude that this product is composed of around 70 wt.% Goethite (metal oxide) and 30 wt.% MWNTs (carbon).

**Morphological properties:** From another side, high resolution microscopy analyses have provide precisely more information about the products textural properties by visualizing the products morphology that affect directly the physico-chemical properties. It is clear that through these micrographs at different resolutions, we can observe the formation of nanofibers (NFs) having a triangular structured base of Goethite, as illustrated in figure (4a'). These nanostructured uni-dimensional forms (1D) have diameters around [181-363 nm] [3]. However, figure (4a) represent FESEM micrograph of selective MWNTs which present homogeneous cylindrical shapes as nested and twisted filament with diameter around 48 nm as generally found in the literature [36, 37].

The following figures (4b and 4b') at two different resolutions show the obtained nanocomposite composed of Goethite and MWNTs where we clearly observe the formation of an assembly of two nanostructured forms, carbon nanotubes and Goethite nanofibers which allow the two nanomaterial properties combination basing on carbon with metal transition oxide.

**Optical characteristics:** Absorption spectra as a function of wavelength in the UV-Vis range [200-1100 nm] for these two products Goethite ( $\text{Fe}_2\text{O}_3 \cdot \text{H}_2\text{O}$ ) and its nanocomposite (Goethite/MWNTs) synthesized by the hydrothermal method are shown in figure 5. They show a remarkable absorbance with absorption peaks around 290 and 375 nm for Goethite and 274, 363 and 491 nm for its nanocomposite with MWNTs. These peaks illustrate the electronic transitions from valence to conduction band.

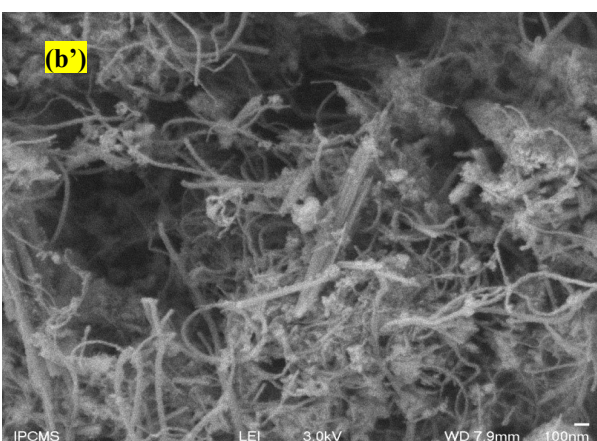
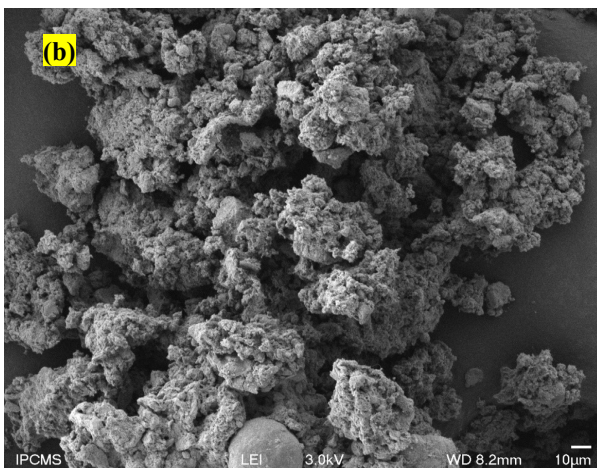
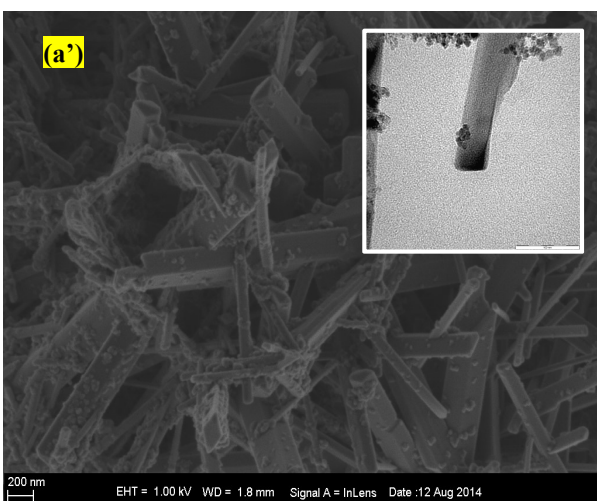
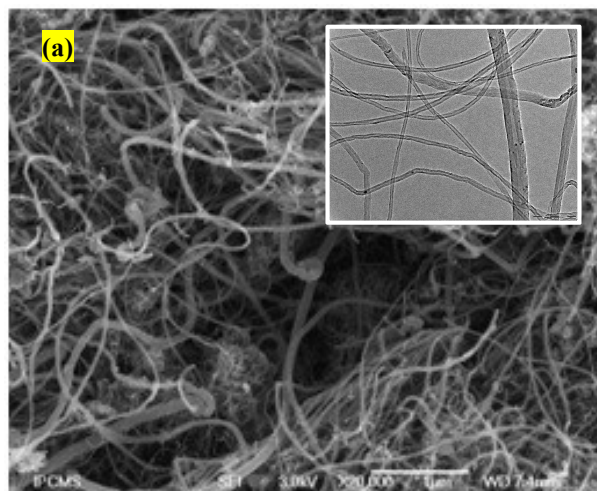


Fig. 4: FESEM micrographs of the obtained MWNTs (a), Goethite based nanofibers (NFs) (a') and their Goethite-NFs/MWNTs nanocomposite (b) and (b') synthesized with hydrothermal process.

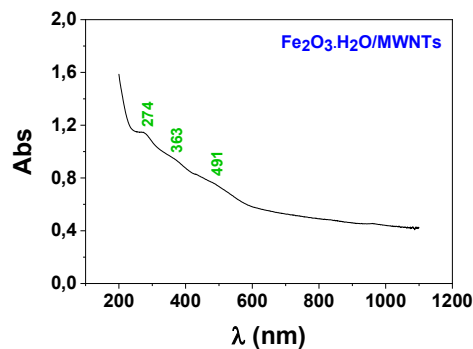
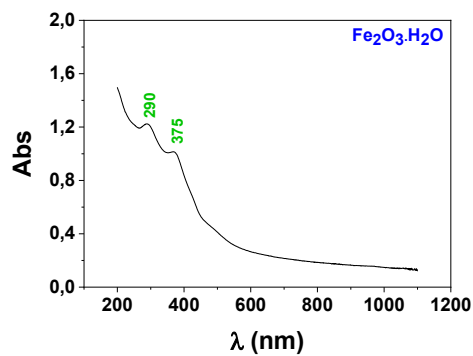


Fig. 5: Absorbance spectra of synthesized Goethite ( $\text{Fe}_2\text{O}_3 \cdot \text{H}_2\text{O}$ ) and its nanocomposite (Goethite/MWNTs) using hydrothermal process.

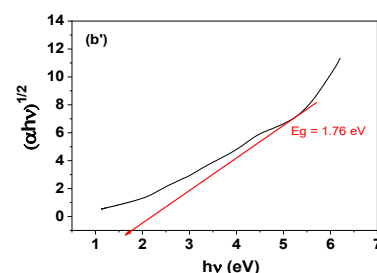
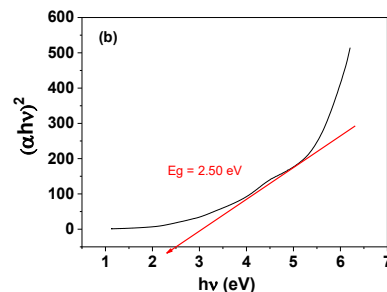
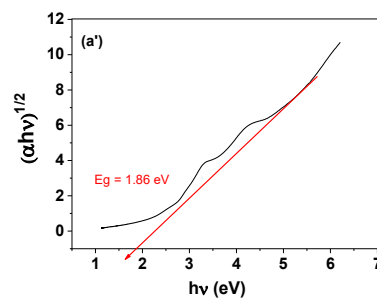
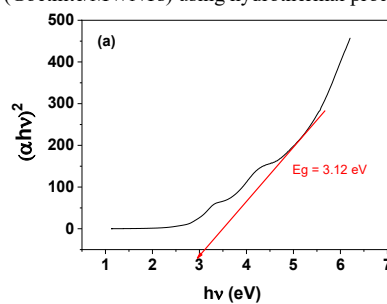


Fig. 6: Gap energy extrapolation for direct and indirect transition in the case of : Goethite (a and a') their nanocomposite Goethite/MWNTs (b and b').

In addition, we have determined the optical gap energy ( $E_g$ ) using the following Tauc equation which can allow the estimation of the nature and the occurrence of electronic transitions [38]:  $(\alpha h\nu)^n = A(h\nu - E_g)$

Where:  $\alpha$  is the absorption coefficient;  $A$  is a constant;  $h\nu$  is the photon energy (eV);  $E_g$  is the band gap energy (eV);  $n$  is a constant which depends on the type of the electronic transition ( $n$  being equal to 2 for direct and 1/2 for indirect transition).

Figure 6 represents the graphic curves of this Tauc equation from the absorption data of these two products in the two suggested cases of electronic transition (direct or indirect transition). Table III regroup their deduced  $E_g$  gap energies for these two cases from these Tauc curves using Origin software (via an extrapolation).

**Table. III**  
DEDUCED GAP ENERGY ( $E_g$ ) FROM TAUC CURVES FOR TWO CASES DIRECT AND INDIRECT ELECTRONIC TRANSITION.

ELECTRONIC TRANSITION	$E_g$ (eV)	
	Goethite ( $\text{Fe}_2\text{O}_3 \cdot \text{H}_2\text{O}$ )	Goethite/MWNTs
DIRECTE	3.12	2.50
INDIRECTE	1.86	1.76

These results clearly indicate that these products are semiconductors with  $E_g < 4$  eV. On the other hand the nanocomposite based on Goethite/MWNTs (70:30 wt.% estimated from TGA analysis) should have a higher electrical conductivity than pure Goethite according to its lower deduced  $E_g$  in comparison to Goethite values; this is in agreement with reported results found in the literature [39].

#### IV. CONCLUSION

In this work, we have studied the experimental results obtained through the synthesis of Goethite hydrated iron oxide and their nanocomposite (Goethite/MWNTs) using hydrothermal process under optimized condition. We identified these products from structural and morphological aspect point of view as well as their thermal and optical properties.

Moreover, these products have shown the formation of Goethite based nanostructured fibers (NFs) with triangular base and carbon-based nanotubes (CNTs) with diameters around 200 nm and 48 nm, respectively, with good dispersion and selectivity.

According to the obtained results, it is confirmed that the addition of MWNTs to iron oxide (Goethite type) significantly improves their physic-chemical properties such as the increase in their electrical conductivity proven by the deduced gap energy  $E_g$  from their absorption of UV-visible light, which is lower in comparison to that of pure iron oxide. On the other hand, there is a degradation in crystallinity/graphitization degree and an increase in the defects as indicated by XRD and Raman spectroscopy analysis, respectively, proved for the last through the  $I_D/I_G$  intensities ratio and the displacement of peaks position.

#### ACKNOWLEDGMENT

We express our gratitude and sincere thanks to Prof. N. Manyala (SARChI) team, Prof. D. Begin (ICPEES) and Prof. F. Antoni (ICub) for their help in FESEM and Raman analysis systems. The authors also thank the Algerian minister program and Directorate General for Scientific Research and

Technological Development (DGRSDT) from Algeria for financial support.

#### REFERENCES

- [1] J. Yang, Y. Liu, S. Liu, L. Li, C. Zhang and T. Liu, "Conducting polymer composites: Material synthesis and applications in electrochemical capacitive energy storage", *Journal of Materials Chemistry Frontiers*, Vol. 1(2), pp. 251–268, 2017. <https://doi.org/10.1039/c6qm00150e>
- [2] M.M. Rahman, P.M. Joy, M.N. Uddin, M.Z. Bin Mukhlis and M.M.R. Khan, "Improvement of capacitive performance of polyaniline based hybrid supercapacitor", *Journal of Heliyon*, Vol. 7(7), pp. e07407, 2021. <https://doi.org/10.1016/j.heliyon.2021.e07407>
- [3] M. Boufas, O. Guellati, A. Harat, D. Momodu, J. Dangbegnon, N. Manyala and M. Guerioune, "Optical and electrochemical properties of iron oxide and hydroxide nanofibers synthesized using new template-free hydrothermal method", *Journal of Nanostructure in Chemistry*, Vol. 10(4), pp. 275–288, 2020. <https://doi.org/10.1007/s40097-020-00348-8>
- [4] M. Manjunatha, R. Kumar, A.V. Anupama, V.B. Khopkar, R. Damle, K.P. Ramesh and B. Sahoo, "XRD, internal field-NMR and Mössbauer spectroscopy study of composition, structure and magnetic properties of iron oxide phases in iron ores", *Journal of Materials Research and Technology*, Vol. 8(2), pp. 2192–2200, 2019. <https://doi.org/10.1016/j.jmrt.2019.01.022>
- [5] A.B. Sengul and E. Asmatulu, "Toxicity of metal and metal oxide nanoparticles", *Journal of Environmental Chemistry Letters*, vol. 18(5), pp. 1659–1683, 2020. <https://doi.org/10.1007/s10311-020-01033-6>
- [6] Q. Feng, Y. Liu, J. Huang, K. Chen, J. Huang and K. Xiao, "Uptake, distribution, clearance, and toxicity of iron oxide nanoparticles with different sizes and coatings", *Journal of Scientific Reports*, Vol. 8(1), pp. 1–13, 2018. <https://doi.org/10.1038/s41598-018-19628-z>
- [7] P. Tartaj, M.P. Morales, T. Gonzalez-Carreño, S. Veintemillas-Verdaguer and C. J. Serna, "The iron oxides strike back: From biomedical applications to energy storage devices and photoelectrochemical water splitting", *Journal of Advanced Materials*, Vol. 23(44), pp. 5243–5249, 2011. <https://doi.org/10.1002/adma.201101368>
- [8] P. Xu, G.M. Zeng, D.L. Huang, C.L. Feng, S. Hu, M.H. Zhao, C. Lai, Z. Wei, C. Huang, G.X. Xie and Z.F. Liu, "Use of iron oxide nanomaterials in wastewater treatment", *Journal of Science of the Total Environment*, Vol. 424, pp. 1–10, 2012. <https://doi.org/10.1016/j.scitotenv.2012.02.023>
- [9] M. Khalid, "Processing and characterization of tailor-made superparamagnetic iron oxide nanoparticles (SPIO-NPs) for pharmaceutical applications", University of Magdeburg Thesis, 2018. <https://141.48.10.209/handle/1981185920/13516>
- [10] Q. Hu, D.Y. Kim, W. Yang, L. Yang, Y. Meng, L. Zhang and H.K. Mao, "FeO<sub>2</sub> and FeOOH under deep lower-mantle conditions and Earth's oxygen-hydrogen cycles treatment", *Journal of Nature*, Vol. 534(7606), pp. 241–244, 2016. <https://doi.org/10.1038/nature18018>
- [11] K. B. Narayanan and S. S. Han, "One-Pot Green Synthesis of Hematite ( $\alpha$ -Fe<sub>2</sub>O<sub>3</sub>) Nanoparticles by Ultrasonic Irradiation and Their In Vitro Cytotoxicity on Human Keratinocytes CRL-2310", *Journal of Cluster Science*, Vol. 27(5), pp. 1763–1775, 2016. <https://doi.org/10.1007/s10876-016-1040-9>
- [12] M. F. Al-Hakkani, G. A. Gouda and S. H. A. Hassan, "A review of green methods for phyto-fabrication of hematite ( $\alpha$ -Fe<sub>2</sub>O<sub>3</sub>) nanoparticles and their characterization, properties, and applications", *Journal of Heliyon*, Vol. 7(1), pp. e0580, 2021. <https://doi.org/10.1016/j.heliyon.2020.e05806>
- [13] Y. H. Chen and C. C. Lin, "Effect of nano-hematite morphology on photocatalytic activity", *Journal of Physics and Chemistry of Minerals*, Vol. 41(10), pp. 727–736, 2014. <https://doi.org/10.1007/s00269-014-0686-9>
- [14] R. A. Revia and M. Zhang, "Magnetite nanoparticles for cancer diagnosis, treatment, and treatment monitoring: Recent advances", *Journal of Materials Today*, Vol. 19(3), pp. 157–168, 2016. <https://doi.org/10.1016/j.mattod.2015.08.022>
- [15] U. S. Khan, Amanullah, A. Manan, N. Khan, A. Mahmood, and A. Rahim, "Transformation mechanism of magnetite nanoparticles", *Journal of Materials Science- Poland*, Vol. 33(2), pp. 278–28, 2015. <https://doi.org/10.1515/msp-2015-0037>
- [16] A.T. Jacobson and M. Fan, "Evaluation of natural goethite on the removal of arsenate and selenite from water", *Journal of Environmental Sciences (China)*, Vol. 76, pp. 133–141, 2019. <https://doi.org/10.1016/j.jes.2018.04.016>
- [17] H. Liu, T. Chen, X. Zou, C. Qing and R. L. Frost, "Thermal treatment of natural goethite: Thermal transformation and physical properties", *Journal of Thermochimica Acta*, Vol. 568, pp. 115–121, 2013. <https://doi.org/10.1016/j.tca.2013.06.027>
- [18] H. Liu, T. Chen and R. L. Frost, "An overview of the role of goethite surfaces in the environment", *Journal of Chemosphere*, Vol. 103, pp. 1–11, 2014. <https://doi.org/10.1016/j.chemosphere.2013.11.065>

- [19] F. Gordon-Núñez, K.Vaca-Escobar, M. García, L.Fernández, A. Debut, M. Sandoval, P. Espinoza-Montero, "Applicability of Goethite/Reduced Graphene Oxide Nanocomposites to Remove Lead from Wastewater", *Journal of nanomaterials*, Vol. 9(11), pp. 1580, 2019. <https://doi.org/10.3390/nano9111580>
- [20] L. Wang, S. Liu, W. Xuan, S. Li, A. Wei, "Efficient Nitrate Adsorption from Groundwater by Biochar-Supported Al-Substituted Goethite", *Journal of sustainability*, Vol. 14, pp.7824, 2022. <https://doi.org/10.3390/su14137824>
- [21] H. Xu, Z. Hu, A. Lu, Y. Hu, L. Li, Y. Yang, Z. Zhang and H. Wu, "Synthesis and super capacitance of goethite/reduced graphene oxide for supercapacitors", *Journal of Materials Chemistry and Physics*, Vol. 141(1), pp. 310–317, 2013. <https://doi.org/10.1016/j.matchemphys.2013.04.048>
- [22] R. Barika, B.K. Jena, A. Dasha, M. Mohapatra, "In-situ synthesis of flowerly shape  $\alpha$ -FeOOH/Fe<sub>2</sub>O<sub>3</sub> nano particles and their phase dependent supercapacitive behaviour". *Journal of The Royal Society of Chemistry*; vol. 1, pp.1–9, 2014. <https://DOI:10.1039/x0xx00000x>
- [23] O. Guellati, S. Detriche, M. Guerioune, Z. Mekhalif and J. Delhalle, "Gas Flow and Temperature Synthesis Dependence on the CNTs structure and yield", *International Journal of Nanoelectronics and Materials*, Vol. 3 (2), p. 125-134, 2010. E ISBN: 2232-1535
- [24] Ö. Güler, "Mechanical and thermal properties of a Cu-CNT composite with carbon nanotubes synthesized by CVD process", *Journal of Material prue fung/Materials Testing*, Vol. 56(9), pp. 662–666, 2014. <https://doi.org/10.3139/120.110615>
- [25] R. Das, S. Hamid, M. Ali, S. Ramakrishna and W. Yongzhi, "Carbon Nanotubes Characterization by X-ray Powder Diffraction – A Review", *Journal of Current Nanoscience*, Vol. 11(1), pp. 23–35, 2014. <https://doi.org/10.2174/1573413710666140818210043>
- [26] N. Debski, "Fibres obtenues a partir de nanotubes de carbone verticalement alignes : élaboration et propriétés", University of South Paris, 2014.
- [27] M. K. Ghosh, G. E. J. Poinern, T. B. Issa and P. Singh, "Arsenic adsorption on goethite nanoparticles produced through hydrazine sulfate assisted synthesis method", *Journal of Chemical Engineering*, Vol. 29(1), pp. 95–102, 2012. <https://doi.org/10.1007/s11814-011-0137-y>
- [28] H. Gupta, R. Kumar, H. S. Park and B. H. Jeon, "Photocatalytic efficiency of iron oxide nanoparticles for the degradation of priority pollutant anthracene", *Journal of Geosystem Engineering*, Vol. 20(1), pp.21–27, 2017. <https://doi.org/10.1080/12269328.2016.1218302>
- [29] K. Hedenstedt, J. Backstr, E. Ahlberg, "In-situ Raman spectroscopy of  $\alpha$ - and  $\gamma$ -FeOOH during cathodic load", *J. Electrochem. Soc.*, Vol. 164(9), pp. H621–H627, 2017. K. Hedenstedt, J. Backstr, E. Ahlberg, "In-situ Raman spectroscopy of  $\alpha$ - and  $\gamma$ -FeOOH during cathodic load", *J. Electrochem. Soc.*, Vol. 164(9), pp. H621–H627, 2017. DOI:10.1149/2.0731709jes
- [30] M. A. Legodi and D. de Waal, "The preparation of magnetite, goethite, hematite and maghemite of pigment quality from mill scale iron waste", *Journal of Dyes and Pigments*, Vol. 74(1), pp.161–168, 2007. <https://doi.org/10.1016/j.dyepig.2006.01.038>
- [31] S. Costa, E. Borowiak-Palen, M. Kruszyńska, A. Bachmatiuk and R.J. Kaleńczuk, "Characterization of carbon nanotubes by Raman spectroscopy", *Journal of Materials Science- Poland*, vol. 26(2), pp.433–441, 2008.
- [32] A. Jorio and R. Saito, "Raman spectroscopy for carbon nanotube applications", *Journal of Applied Physics*, Vol. 129(2), 2021. <https://doi.org/10.1063/5.0030809>
- [33] R. G. Abaszade, O. A. Kapush and A. M. Nabiev, "Properties of carbon nanotubes doped with gadolinium", *Journal of Optoelectronic and Biomedical Materials*, Vol. 12(3), pp.61–65, 2020.
- [34] O. Guellati, D. Bégin, F. Antoni, S. Moldovan, M. Guerioune, C. Pham-Huu, I. Janowska, "CNTs' array growth using the floating catalyst-CVD method over different substrates and varying hydrogen supply", *Mater. Sci. Eng. B Solid-State Mater. Adv. Technol.* Vol. 231, pp. 11-17, 2018. <https://doi.org/10.1016/j.mseb.2018.03.001>
- [35] V.P. Ponomar, "Thermomagnetic properties of the goethite transformation during high-temperature treatment", *Journal of Materials Minerals Engineering*, Vol. 127 (August), pp. 143–152, 2018. <https://doi.org/10.1016/j.mineng.2018.08.016>
- [36] S. Lagoutte, P. H. Aubert, M. Pinault, F. Tran-Van, M. Mayne-L'Hermite and C. Chevrot, "Poly(3-methylthiophene)/vertically aligned multi-walled carbon nanotubes: Electrochemical synthesis, characterizations and electrochemical storage properties in ionic liquids", *Journal of Electrochimica Acta*, Vol. 130, pp. 754–765, 2014. <https://doi.org/10.1016/j.electacta.2014.03.097>
- [37] C. Castro, M. Pinault, D. Porterat, C. Reynaud, and M. Mayne-L'Hermite, "The role of hydrogen in the aerosol-assisted chemical vapor deposition process in producing thin and densely packed vertically aligned carbon nanotubes", *Journal of Carbon*, Vol. 61, pp. 585–594, 2013. <https://doi.org/10.1016/j.carbon.2013.05.040>
- [38] A. Lassoued, B. Dkhil, A. Gadri and S. Ammar, "Control of the shape and size of iron oxide ( $\alpha$ -Fe<sub>2</sub>O<sub>3</sub>) nanoparticles synthesized through the chemical precipitation method", *Journal of Results in Physics*, Vol.7, pp.3007–3015, 2017. <https://doi.org/10.1016/j.rinp.2017.07.066>
- [39] C. Bao, X. Liu, X. Shao, X. Ren, Y. Zhang, X. Sun, D. Fan, Q. We and H. Ju, "Cardiac troponin I photoelectrochemical sensor: {Mo368} as electrode donor for Bi2S3 and Au co-sensitized FeOOH composite", *Journal of Biosensors and Bioelectronics*, Vol.157(March), pp.112–157, 2020. <https://doi.org/10.1016/j.bios.2020.112157>

**Sara DJELAMDA** Phd in Applied physics, Domain of research: Nanocomposite, Polyaniline, In-situ growth, energy storage.



**Ouanassa Guellati**, permanent researcher in LEREC laboratory in Algeria and Teacher at Souk-Ahras University, has completed her PhD from Badji-Mokhtar University of Annaba 2013, Algeria on production of Carbon nanotube (CNTs) using CCVD technique and their functionalization and macronisation. She has published 23 papers in reputed journals with high impact factor. She has presented in september 2020 her university habilitation at Badji-Mokhtar University of Annaba. She is current reviewer in *Nanoscale Research Letters* and *Materials Science and Engineering B – Journal Elsevier*. Actually, she is working on the production of smart nanomaterials like transition metal hydroxides, oxides and nanostructured polyaniline and their nanocomposites / nanohybrids with CNTs and/or Graphene as well as mesoporous Biochars for energy storage, environment and Biosensing application. She is working in collaboration with ICPEES at ECPM, Strasbourg – France, IMS at University of Valencia – Spain, CES at Namur University, SARChI Chair in Carbon Technology and Materials at Pretoria University, South Africa and DISAT - Politecnico di Torino, Italy.

